

ROLE OF CLIMATE IN GLOBAL CHANGE – FROM MILANKOVITCH'S TIME UNTIL END OF THE 21ST CENTURY SLOBODAN P. SIMONOVIC

*The University of Western Ontario, Department of Civil and Environmental Engineering,
London, Ontario, Canada
E-mail: simonovic@uwo.ca*

Abstract. The focus of this paper is on the role climate change is playing in global change. Feedbacks play key roles in Earth's short-term weather and long-term climate. Milutin Milankovitch developed a theory that the long-term, collective effects of changes in Earth's position relative to the Sun are a strong driver of Earth's long-term climate. Milankovitch cycles provide a strong framework for understanding long-term changes in Earth's climate. They cannot account for the current period of rapid warming. Presented work is based on the global assessment model ANEMI which is using as the main driver of climate change the greenhouse gas emissions, which are in turn driven by energy consumption from a growing population. Set of simulation experiments with the model confirms that climate plays an important role in the performance of Earth system. The future integration of long term climate change impacts (Milankovitch cycles) and short term drivers (greenhouse gasses emissions) will provide deeper understanding of the climate impacts on global change and guide future mitigation and adaptation actions.

Key words: Milutin Milanković, Global Change, Climate Change, System Dynamics, Modelling

Apstrakt. Fokus ovog rada jeste uloga klimatskih promena u globalnim promenama. Povratne informacije igraju ključnu ulogu u kratkoročnom vremenu i dugoročnoj klimi Zemlje. Milutin Milanković razvio je teoriju po kojoj dugoročni, ukupni uticaji promena Zemljinog položaja u odnosu na Sunce jesu snažan pokretač Zemljine dugoročne klime. Milankovićevi ciklusi pružaju bitan okvir za razumevanje dugoročnih promena klime Zemlje. Ciklusi ne mogu da budu odgovorni za trenutno ubrzano globalno zagrevanje. Ovaj rad je utemeljen na globalnom modelu procene ANEMI koji koristi glavni pokretač klimatskih promena, gasove sa efektom staklene bašte, koji su, pak, uslovljeni korišćenjem energije od sve više rastućeg globalnog stanovništva. Set simulirajućih eksperimenata sa modelom potvrđuju da je uloga klime u radu Zemljinog sistema izuzetna. Buduća integracija dugoročnih uticaja klimatskih promena (Milankovićevi ciklusi) i kratkoročnih pokretača (gasovi sa efektom staklene bašte) obezbediće dublje razumevanje uticaja klime na globalne promene i vodiće buduća delovanja radi otklanjanja i prilagođavanja istim.

Ključne reči: Milutin Milanković, globalne promene, klimatske promene, dinamika sistema, modeliranje

1. INTRODUCTION

Global change is being realized as a close consequence of changing climate, creating the need to consider environmental problems and their interactions with the Earth as a system. The Earth system is composed of biological, physical, chemical, and human elements that form a network of feedbacks through their interconnections. The concept of global change becomes increasingly important as the components of the Earth system such as population, economic productivity, climate, food production, and hydrology are interlinked through dynamic non-linear feedback processes. Within this system, changes in one component inevitably lead to changes in another. The society-biosphere-climate model presented here takes an integrated assessment approach to simulating global change. It consists of eleven individual sectors that reproduce the main characteristics of the climate, carbon cycle, energy - economy, land use, food production, persistent pollution, population, hydrologic cycle, water demand, water supply and water quality sectors at a global scale [1, 2, 3].

The focus of this presentation is on the role climate change is playing in global change. Feedbacks play key roles in Earth's short-term weather and long-term climate. A century ago, Serbian scientist Milutin

Milankovitch [4] developed a theory that the long-term, collective effects of changes in Earth's position relative to the Sun are a strong driver of Earth's long-term climate, and are responsible for triggering the beginning and end of glaciation periods (Ice Ages). Specifically, he examined how variations in three types of Earth orbital movements affect how much solar radiation (known as insolation) reaches the top of Earth's atmosphere as well as where the insolation reaches. These cyclical orbital movements, which became known as the „Milankovitch cycles“, cause variations of up to 25 percent in the amount of incoming insolation at Earth's mid-latitudes (the areas of our planet located between about 30 and 60 degrees north and south of the equator). Milankovitch cycles provide a strong framework for understanding long-term changes in Earth's climate. They cannot account for the current period of rapid warming Earth has experienced since the pre-Industrial period (the period between 1850 and 1900), and particularly since the mid-20th Century. Milankovitch cycles operate on long time scales, ranging from tens of thousands to hundreds of thousands of years. In contrast, Earth's current warming has taken place over time scales of decades to centuries. However, Milankovitch cycles are one important factor that contributes to climate change, both past and present.

Presented work is based on the global assessment model ANEMI [1, 2, 3] which is implemented in a system dynamics modelling interface called Vensim DSS [5], which emphasizes the roles of nonlinearity and feedback in determining system behaviour. ANEMI model climate sector is discussed in details after introduction of the model (Section 2) and use of the model to investigate the role of climate change in global change (Section 3). The paper ends with concluding comments in Section 4.

2. ANEMI GLOBAL ASSESSMENT MODEL

This chapter presents the ANEMI model, which is currently in version 3 [3], built upon the first two iterations of ANEMI [1, 2]. The model shares the same system dynamics simulation paradigm that was used in the previous iterations of ANEMI, in that feedbacks and delays are used to drive system behaviour. ANEMI3 is a type of integrated assessment model that describes the state of and interactions between model sub-systems that compose the Earth system. The main sub-systems or 'sectors' used are that of the climate system, carbon, nutrient, and hydrologic cycles, population dynamics, land use, food production, sea level rise, energy production, global economy, persistent pollution, water demand, and water supply development.

2.1 ANEMI model structure

Each individual sector in the model describes the relevant feedbacks that drive the state variables in the sector. Connections between sectors form intersectoral feedbacks responsible for the functioning of the Earth system. It is the intersectoral feedbacks that allow us to represent feedbacks that drive global changes in the Earth system. Feedbacks driving global change are now evident, while it is expected that negative feedbacks acting on population and economic growth may be more evident in the future. From a system dynamics perspective, effective policymaking should be based on addressing the feedback structure of a system, not only on modifying the system parameters. This viewpoint is what makes the ANEMI3 model unique and useful in a time when global modelling is becoming progressively more complex.

The boundary of the model is defined by the problem that is being explored. In this paper, we are modelling the role of climate in various aspects of global change. Therefore, the spatial scale of the model is mainly one that is global. In some sectors, the stocks are disaggregated to capture material flows on a sub-global scale, but not at a level that is location specific. This spatial scale limits the level of detail that can be used to describe the flows that act to change the model stocks, however it allows us to effectively analyze feedbacks between water resources and other model sectors on a global scale.

The highly endogenous structure and coupling of sub-systems in the ANEMI3 model are part of its novelty in the realm of integrated assessment modelling. Because of this, feedback processes are responsible for the behaviour that is exhibited in model runs. The model sectors that comprise the ANEMI3 model are that of the climate system, carbon, nutrient, and hydrologic cycles, population dynamics, land use, food production, sea level rise, energy production, global economy, persistent pollution, water demand, and water supply development as shown in Figure 1. Feedback loops between sectors, or intersectoral feedback loops are responsible for global change in this Earth system. Intersectoral feedbacks in the ANEMI3 model allow for the representation of various aspects of global change. In the Figure 1 diagram alone there is a total of 89

[Type here]

possible intersectoral feedback loops. The size of the feedback loops range from 2 to 9 sectors included out of the 10 that are shown. Creating a causal loop diagram from these connections between model sectors allows us to view the feedbacks that are created by combining model sectors in this way.

2.1 ANEMI model climate sector

The climate sector of ANEMI3, as in previous versions, is based on the DICE model of Nordhaus [6]. In this sector, the dynamics of heat exchange between the deep ocean and the combined upper ocean and atmospheric layers are modelled, along with a cooling effect that acts to limit the rate of temperature increase. Identifying the feedbacks that drive this simple climate system allow us to speculate on how the system will function over time. Error: Reference source not found The climate sub-system is driven by two feedback loops (Error: Reference source not found). The first being a feedback cooling effect, while the second represents the diffusion of heat in the atmospheric stock to the ocean stock. Both of these negative feedbacks act to dampen the systems response to radiative forcing which comes from increased greenhouse gas concentrations in the carbon cycle and greenhouse gas sub-systems. Based on the structure of this simplified climate system, one might expect it to predict global temperature values on the lower end of the spectrum. This is because positive feedbacks related to climate change such as methane release from tundra regions and change in albedo as global ice cover melts are not

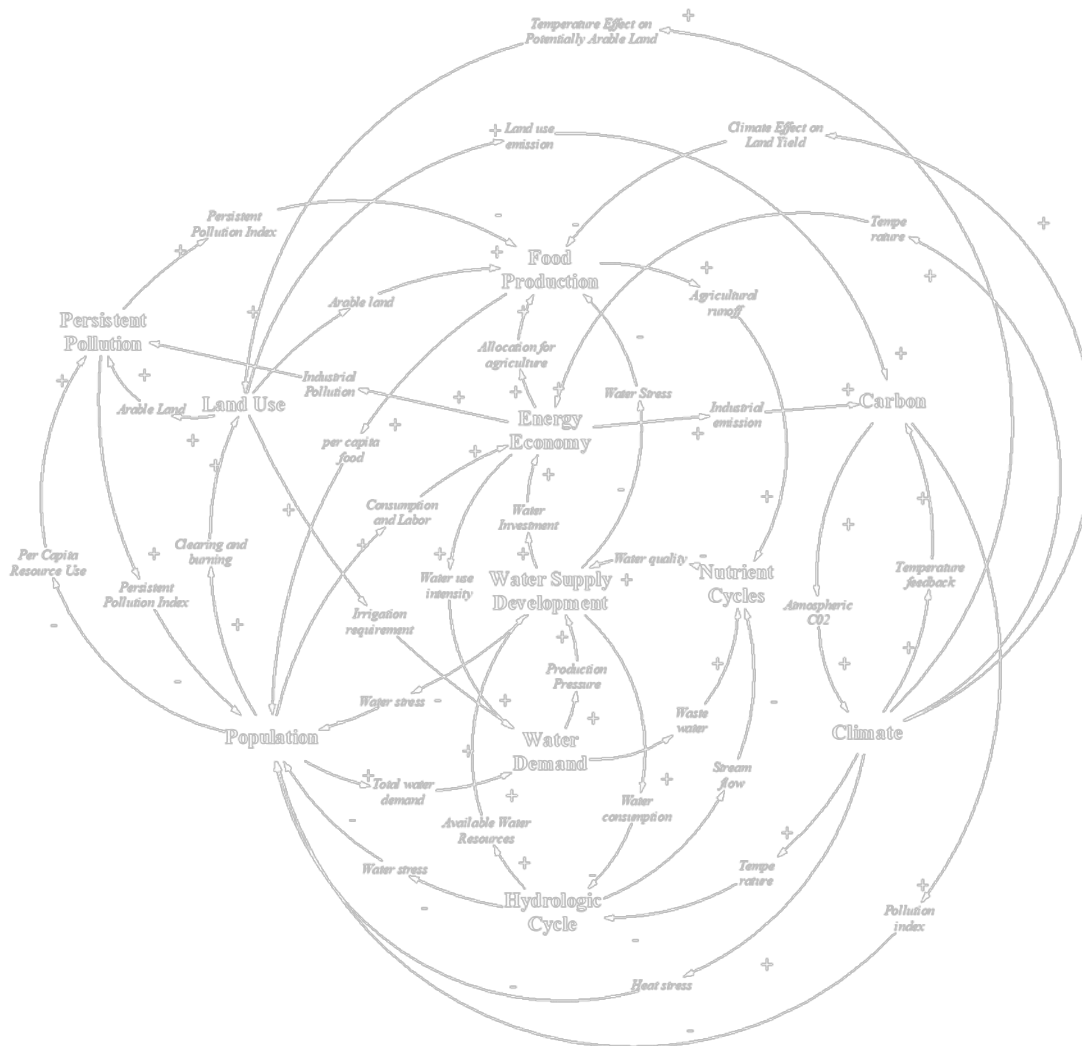


Fig. 1 High-level feedback structure of the ANEMI3 model illustrated as a causal loop diagram

included, which have the potential to accelerate increases in global temperatures.

The stock and flow diagram of this model is given in Fig. 3 Two stocks are used to quantify the current global temperature of the atmosphere and oceans in response to external radiative forcing caused by greenhouse gases that are divided into CO₂, methane, nitrogen dioxide, chlorofluorocarbons, and others. Diffusion of heat between these two stocks results in heat being transferred from the atmosphere stock to the ocean stock which acts as a heat sink.

Radiative forcing acts to increase the flow that changes the temperature of the atmosphere stock and is based on the relative change of the greenhouse gases considered from their preindustrial levels. The mathematical description of the atmospheric and upper ocean temperature stock is given by,

$$T_{AUO} = \int CT_{AUO} \cdot dt \quad [^{\circ}C] \tag{1}$$

where T_{AUO} represents the temperature of the atmosphere and upper ocean and CT_{AUO} is the rate at which T_{AUO} is changing ($^{\circ}C/year$).

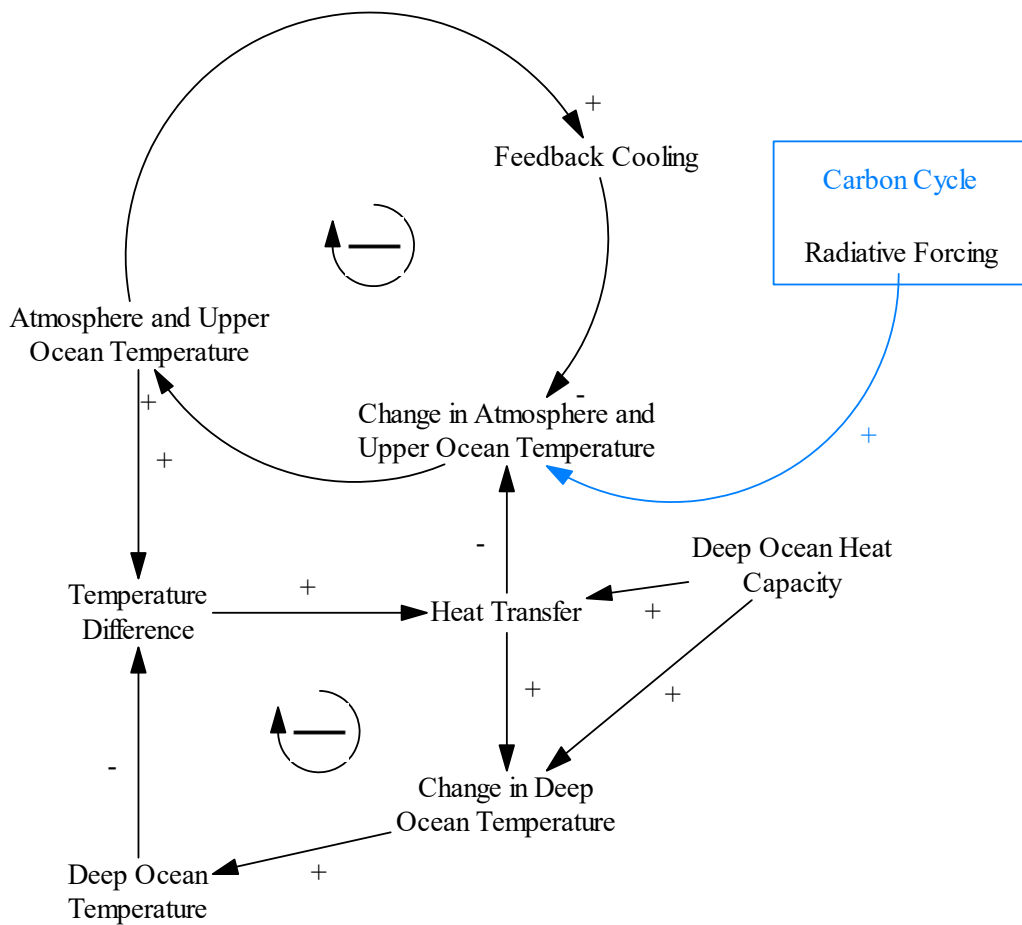


Fig. 2 Causal loop diagram of the ANEMI3 climate sector.

[Type here]

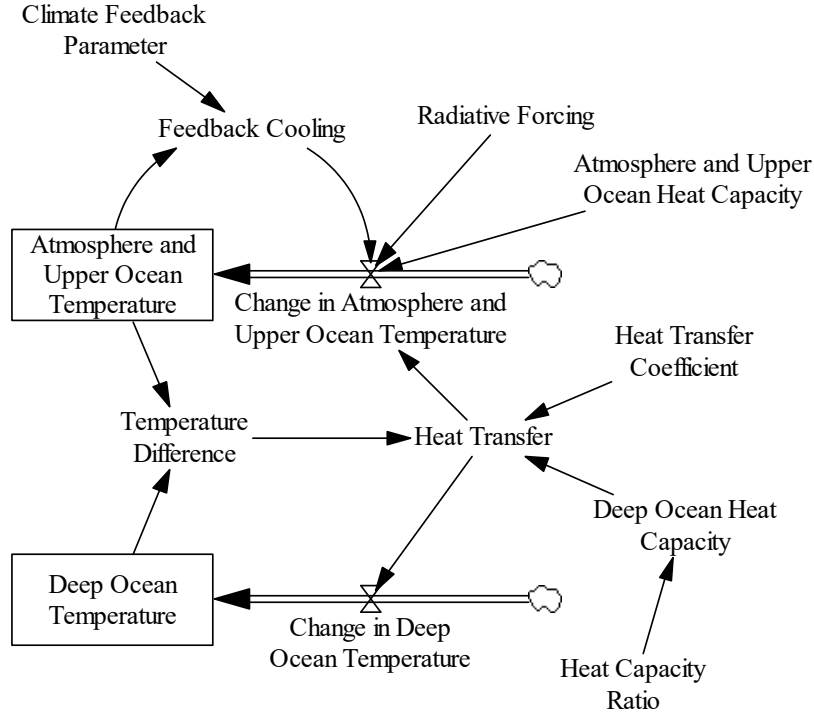


Fig. 3 Stock and flow diagram of the ANEMI3 climate sector.

The deep ocean temperature, T_{DO} is defined as,

$$T_{DO} = \int CT_{DO} \cdot dt \quad [^{\circ}C] \quad (2)$$

where CT_{DO} is the change in temperature of the deep ocean stock ($^{\circ}C/year$). The change in temperature of the atmospheric and upper ocean stock is calculated based on the difference between radiative forcing, heat transfer from the deep ocean stock and the heat capacity of the atmospheric and upper ocean stock,

$$CT_{AUO} = \frac{F - f_H - HT}{HC_{AUO}} \quad [^{\circ}C/year] \quad (3)$$

where:

$F =$ Radiative forcing [W/m^2]

$f_H =$ Feedback cooling effect [W/m^2]

$HT =$ Heat transfer between atmosphere and upper ocean to deep ocean [W/m^2]

$HC_{AUO} =$ Heat capacity of atmosphere and upper ocean [$W \cdot \frac{year}{^{\circ}C \cdot m^2}$]

The change in temperature of the deep ocean stock, CT_{DO} depends on the heat transfer from the atmosphere and upper ocean layer above, and the heat capacity of the deep ocean stock,

$$CT_{DO} = \frac{HT}{HC_{DO}} \quad [^{\circ}C/year] \quad (4)$$

where:

HC_{DO} = Heat capacity of deep ocean layer [$W \cdot \frac{year}{^{\circ}C \cdot m^2}$]

Heat capacity of the deep ocean layer is calculated by,

$$HC_{DO} = R_{HC} \cdot C_{HT} \quad \left[W \cdot \frac{year}{^{\circ}C \cdot m^2} \right] \quad (5)$$

where:

R_{HC} = Heat capacity ratio [$W/(m^2 \cdot ^{\circ}C)$]

C_{HT} = Heat transfer coefficient [year]

The transfer of heat between the atmosphere and upper ocean and deep ocean layers is dependent upon the difference in temperature between them, the heat capacity of the deep ocean layer and heat transfer coefficient.

$$HT = (T_{AUO} - T_{DO}) \frac{HC_{DO}}{C_{HT}} \quad [W/m^2] \quad (6)$$

3. ROLE OF CLIMATE IN GLOBAL CHANGE

Climate change is likely to raise the global average temperature by over 2 degrees C by the year 2100 relative to the 1850-1900 period [7]. As a result, water in the hydrologic cycle is expected to move faster resulting in more extreme and frequent rainfall and streamflow. As ocean temperature rises more moisture will enter the atmosphere resulting in greater amounts of rainfall on land on average. Therefore, there will be more available surface water in total, but potentially less available water in time and space for human use due to the expected shifts in global rainfall patterns. Increased surface temperatures are also expected to be linked to more frequent and severe heat waves that have the potential to increase mortality rates in young and elderly demographics in certain areas of the World. In addition, more areas will become feasible for new agriculture [8], potentially allowing for greater food production.

3.1 ANEMI model performance

Many of the variables in ANEMI3 do not have historically observed counter parts on a global scale, but there are key variables in each sector that can be compared to historical data. One thing to note in this comparison is that on a global scale, there are many datasets that are incomplete (data is only recorded for certain regions), inconsistent (different recording methodologies used across regions, recording is done at irregular intervals), and at times, unreliable. However, there is still value in comparing the model to the real world in any way possible to see that it reproduces the behaviour of the sub-systems that are being represented. Note that the goal is not to reproduce the numbers from the data, but build confidence in the model's ability to generate realistic system behaviours in order to build confidence in future behaviours that arise, as well as policies that are implemented to alter them.

For baseline model comparison and climate sector performance assessment the NASA [9] global atmospheric temperature data are used. The variation in global temperatures due to climate change from the year 1980 are shown in Figure 4. From 1980 to 2018 the ANEMI3 model predicts a global temperature change of 0.87 degrees, while the observed NASA data reports a value of 0.6 degrees. The simplified climate system in ANEMI3 is not able or designed to capture the annual variation in global temperatures that are present in the observed NASA data. The behavioural mode is similar, with a slightly higher slope obtained by the ANEMI3. More comparisons are made in Section 4.1.1 with regards to projected change in global

[Type here]

temperature change.

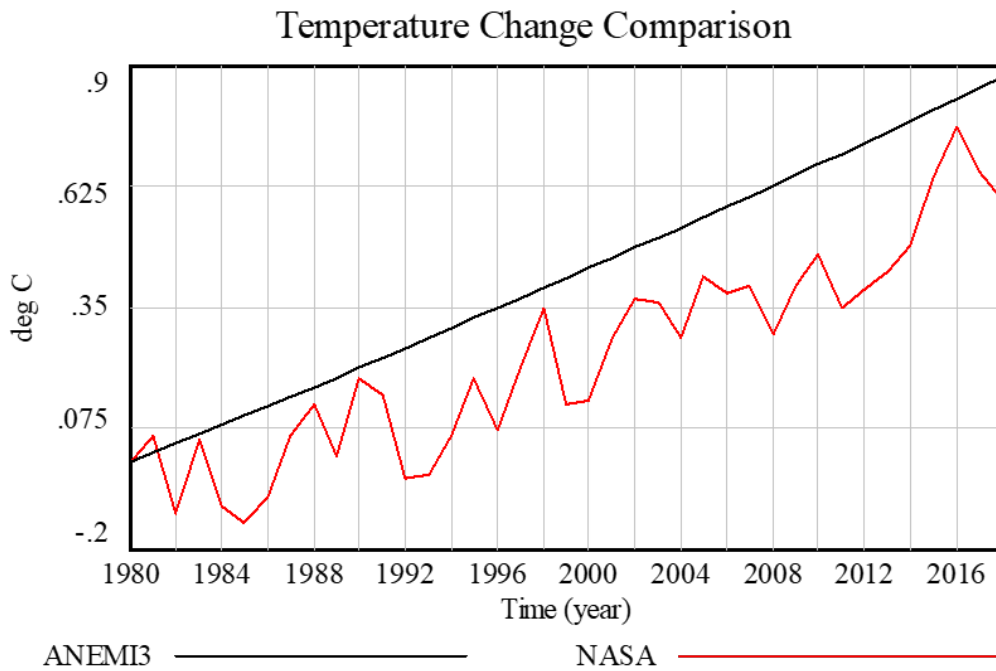


Fig. 4 Global temperature change from 1980-2018 comparison between ANEMIS3 climate sector and NASA observed data.

3.2 Impacts of climate change on the Earth system

In this section the impacts of climate change on various components of the Earth system are explored. The main driver of climate change in the Earth system are greenhouse gas emissions, which are in turn driven by energy consumption from a growing population. For better understanding of interconnected structure of the model and Earth system performance Figure 5 presents the trajectories of the main stocks in the baseline scenario that define the state of the ANEMIS3 model.

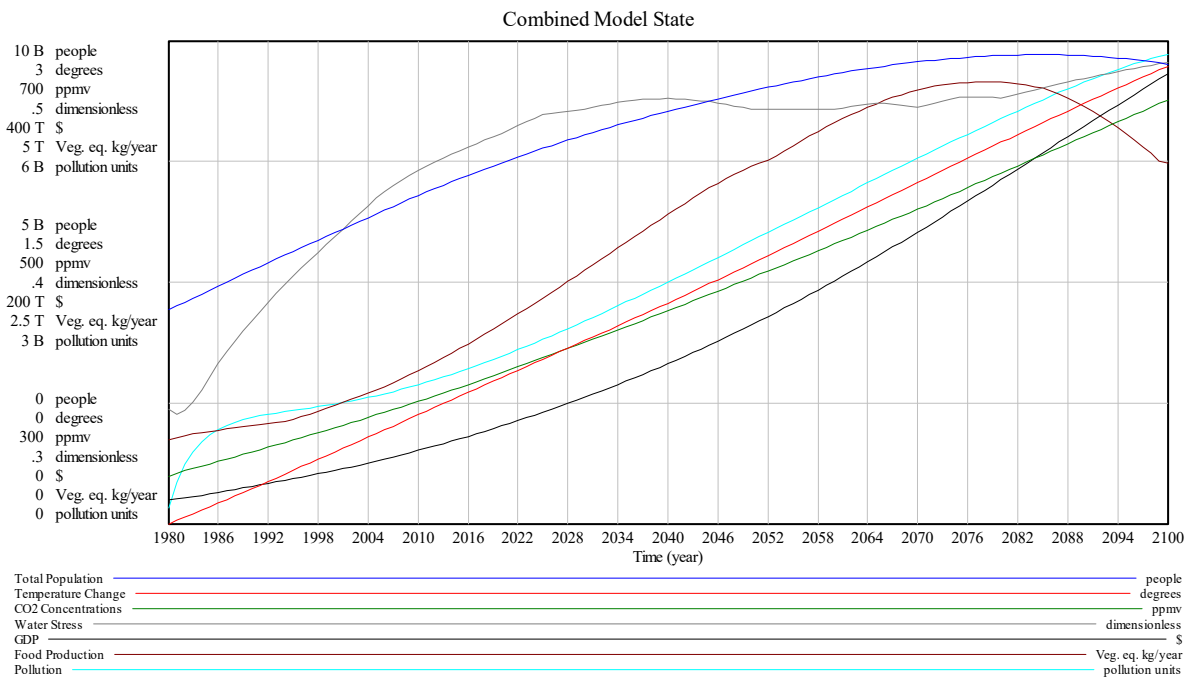


Fig 5 ANEMIS3 model performance for the period 1980 - 2100.

The change in global atmospheric temperatures follows an almost linear path (red line in Figure 5), reaching a change of almost 3 degrees by the year 2100. This is due to increasing CO₂ levels, which start at an atmospheric concentration of 339 ppm and rise to 650 ppm. This corresponds to an increase of 1.9 times. The ANEMI3 model was run with the emissions scenarios for the greenhouse gases of carbon dioxide, methane, nitrogen dioxide, and chlorofluorocarbons from the fifth assessment report of the IPCC in order to compare the resulting temperature changes from the different RCP scenarios [10]. Each of the RCP scenarios represents a different socioeconomic pathway for greenhouse gas emissions and are defined by the total radiative forcing on the climate system at the end of the century. For example, RCP4.5 represents a socioeconomic pathway for emissions resulting in a total radiative forcing of 4.5W/m² by the year 2100. The socioeconomic pathways embedded in each RCP scenario contain projections of population, GDP, energy production, and land use. Comparing the differences in global surface temperatures projected from the ANEMI3 baseline to those projected from the RCPs allows for a much more general comparison of where the over socioeconomic pathway of ANEMI stands.

The change in global surface temperatures resulting from running the ANEMI3 model with the RCP scenarios, is shown in Figure 6. The ANEMI3 results are found to be within what is projected with the RCP scenarios, between those of RCP6 (2.6°C by 2100) and RCP8.5 (4.3°C by 2100) corresponding to a 2.7°C temperature change by the year 2100. Comparing the CO₂ concentrations of the RCP scenarios to that of the ANEMI3 model also shows a similar result, with a very close trajectory to RCP6. This indicates that the overall socioeconomic pathway of the ANEMI3 baseline run is between one that is medium to high in terms of emissions with some climate change mitigation present.

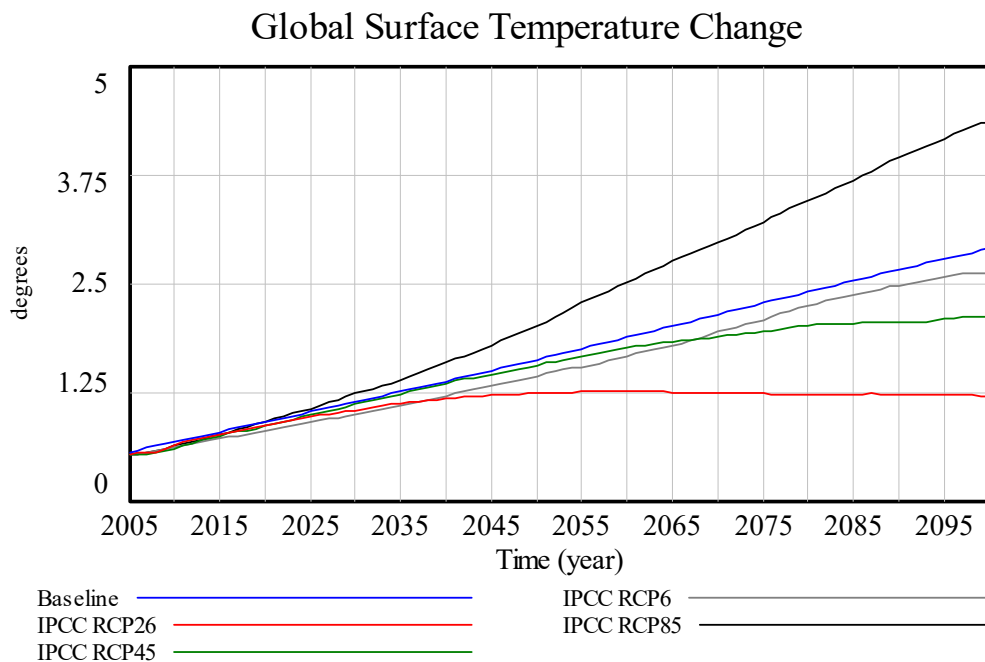


Fig 6 Global surface temperature change comparison between ANEMI3 baseline and ANEMI3 running with the RCP scenario GHG emissions

In this section the impacts of climate change on various components of the Earth system are explored. The main driver of climate change in the Earth system are greenhouse gas emissions, which are in turn driven by energy consumption from a growing population. In order to examine the range of global impacts due to climate change in the model, the RCP emissions scenarios are used and compared to the ANEMI3 baseline. This will allow for a range of climate change effects from changes in global surface temperature and precipitation to be examined.

Global surface temperature changes resulting from the RCP greenhouse gas emission scenarios are shown in Figure 6. The resulting range of global surface temperature change is between 2 to 4.4 degrees by the year 2100. The temperature change in the RCP2.6 scenario shows an increase in temperature until the year 2060,

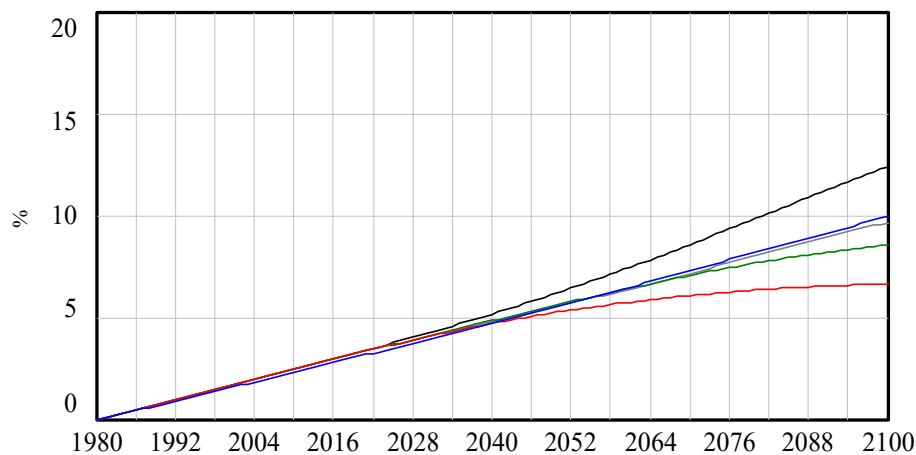
[Type here]

after which temperatures slightly decrease. The RCP8.5 scenario is increasing almost linearly after the year 2045 until the year 2100. The changes in global surface temperatures are used in the hydrologic cycle of the ANEMI3 model to drive changes in precipitation amounts for rainfall and snowfall, as well as evapotranspiration and available surface water (Figure 7).

Increases in global surface temperatures result in changes in precipitation amounts ranging from 11 to 16.5%, with the largest changes occurring for the RCP8.5 scenario. This is due to reduced amounts of snowfall on the land surface, as well as increase in ocean evaporation and evapotranspiration. Evapotranspiration increases between 7 and 13% as a result of increase in surface temperatures. The combined effect results in more available surface water from increase in streamflow ranging from 15,602 to 16,000 km³/year by 2100 up from the initial value of 15,240 km³/year. In the case of RCP2.6 the amount of available surface water decreases slightly after the year 2070 when the climate change signal is not as strong, however global surface temperature is still increasing slightly at this point (Figure 6). This is due to human consumption having a negative effect on available surface water, although the influence of climate on a global scale has a larger impact on the net result.

The effect of climate change on the net arable land is shown in Figure 8a. Overall, all climate change scenarios have a positive effect on net arable land, with an increase ranging from 0.5 to 0.8 billion hectares. This is because of increased arable land through conversion of boreal forests to agriculture as temperature increases (Figure 8b), along with the impacts of sea level rise on agricultural land (Figure 8c). Although sea level rise removes arable land from the net value as agricultural areas become inundated, the effect of utilizing new potentially arable land as a result of warmer climates in northerly regions is dominating. The land yield rates affect the amount of food that is produced from the net amount of arable land in the model (Figure 8d). In all climate change scenarios, land yield is reduced significantly via increase in global surface temperature as a result of heat stress.

Change in Rainfall Amounts with Climate



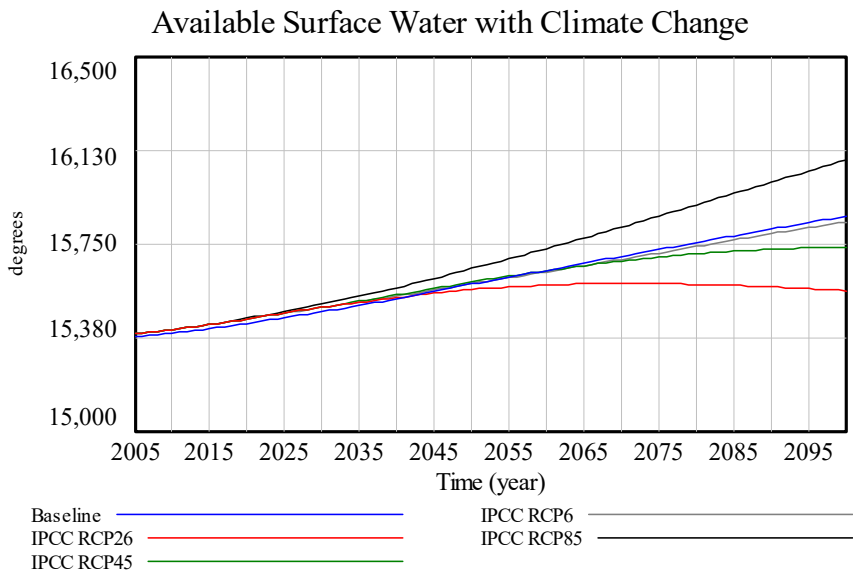
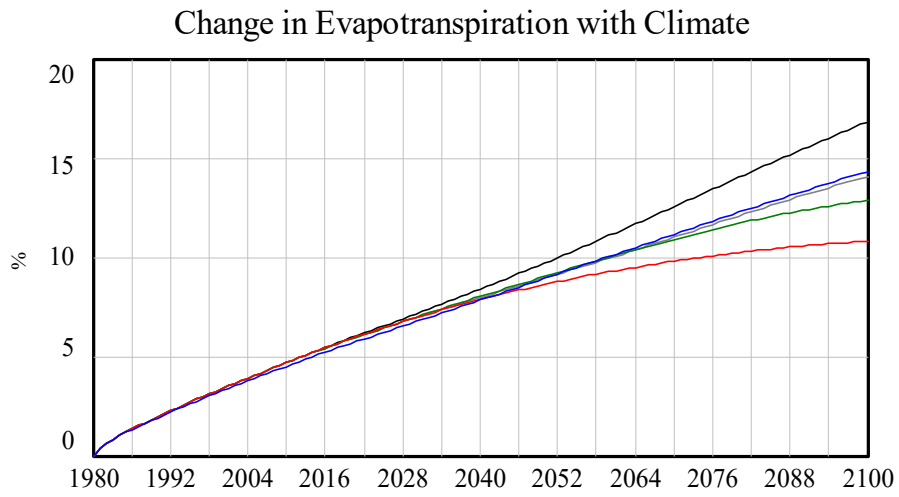


Fig 7 Changes of precipitation, evapotranspiration, and available surface water with five climate change scenarios.

[Type here]

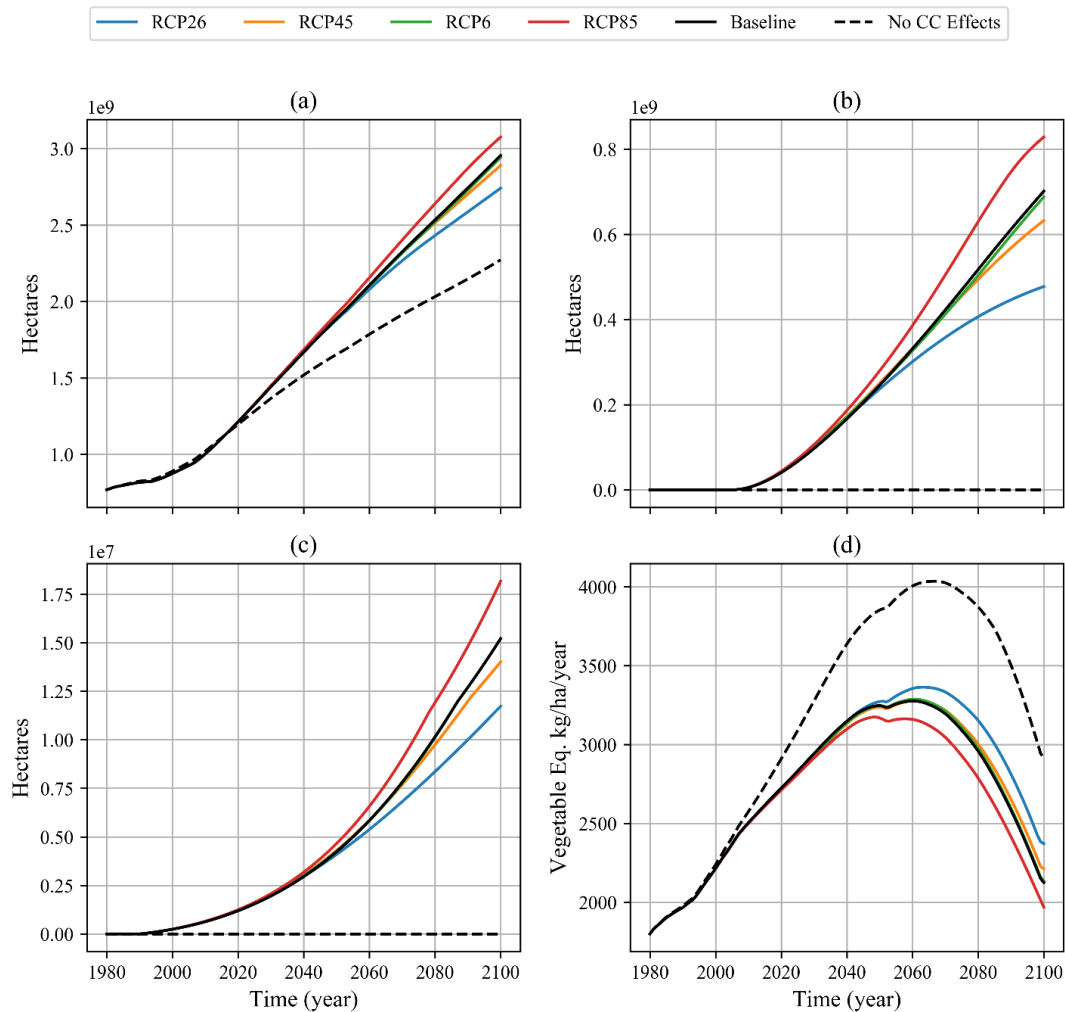


Fig 8 Effect of climate change on (a) net arable land and factors affecting food production including (b) increase in arable land through boreal forest conversion, (c) impacted agricultural land by the sea level rise, and (d) land yield.

The net effect of climate change on food production including changes in net arable land from sea level rise and arable land expansion, and land yield is shown in Figure 9. Considering all of the climate change effects included in the ANEMI3 model on food production, the result is a net decrease in food production corresponding to a maximum of 9% when comparing the RCP8.5 scenario to the scenario with no climate change effects applied. Climate change effects on land yield and net arable land balance themselves to a degree, but in this case the effects of reduced land yield are slightly stronger. It should be noted that there are uncertainties, spatial variations, and climate change effects that are not considered here. The food production in ANEMI3 overtime shows a behaviour mode of overshoot and collapse in all scenarios.

Economic impact of climate change and its effect on global economic output is represented by the climate damage function in the ANEMI3 model, shown in Figure 10. The climate damage multiplier (functions in Figure 10) for representing the impact on economic output varies from 1 (no climate impact) in 1980 to a range between 0.994 and 0.981 for RCP2.6 and RCP8.5 climate scenarios in 2100, respectively. This represents almost a 2% reduction in global economic output per year, which corresponds to a value of 7.6 trillion 1980 US\$ for the RCP8.5 scenario. Under the RCP2.6 scenario, climate damages appear to level off by the year 2100, however in the case of RCP8.5 the negative slope is increasing. The baseline scenario follows a pathway that is almost identical to RCP6. This is due to the temperature changes being nearly the same between the ANEMI baseline and RCP6 scenario.

4. CONCLUSIONS

Milankovitch cycles provide a strong framework for understanding long-term changes in Earth's climate. They cannot account for the current period of rapid warming Earth has experienced since the pre-Industrial

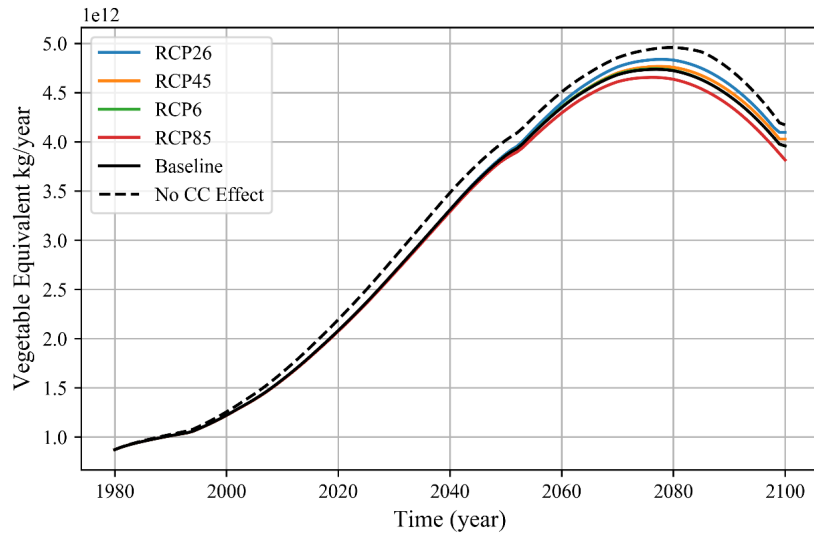
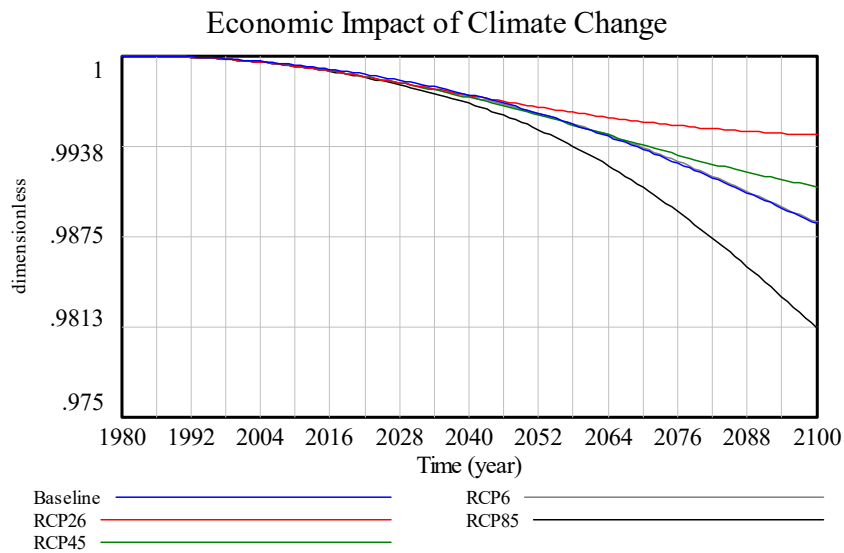


Fig 9 Net effect of climate change on food production including the effects of changes in net arable land and land yields.



Fi 10 Climate damage functions.

period (the period between 1850 and 1900), and particularly since the mid-20th Century. Milankovitch cycles operate on long time scales, ranging from tens of thousands to hundreds of thousands of years. However, Milankovitch cycles are one important factor that contributes to climate change, both past and present.

Presented work is based on the global assessment model ANEMI [1, 2, 3] which is using as the main driver of climate change the greenhouse gas emissions, which are in turn driven by energy consumption from a growing population. Set of simulation experiments with the model confirms that climate plays an important role in the performance of Earth system.

The future integration of long term climate change impacts (Milankovitch cycles) and short term drivers (green house gasses emissions) will provide deeper understanding of the climate impacts on global change and guide future mitigation and adaptation actions.

[Type here]

-4. ACKNOWLEDGMENTS

Work presented in this paper is funded by the discovery grant from the Natural Sciences and Engineering Research Council of Canada.

5. REFERENCES

1. Davies EGR, Simonovic SP. , 2010. ANEMI: a new model for integrated assessment of global change. *Interdiscip Environ Rev.*, 11: 127–161. doi:10.1504/IER.2010.037903
2. Akhtar MK, Wibe J, Simonovic SP, Macgee J., 2013. Integrated assessment model of society-biosphere-climate-economy- energy system. *Environ Model Softw.*, 49: 1–21. doi:10.1016/j.envsoft.2013.07.006
3. Breach PA, Simonovic SP., 2020. ANEMI3: Tool for investigating impacts of global change. *Water Resources Research Report* no. 108, Facility for Intelligent Decision Support, Department of Civil and Environmental Engineering, London, Ontario, Canada, 134 pages. ISBN:978-0-7714-3146-3.
4. Milankovitch, M., 1920. Théorie mathématique des phénomènes thermiques produits par la radiation solaire, XVI, 338 S. – Paris: Gauthier-Villars.
5. Ventana Systems, 2003. *Vensim DSS Software*. Ventana Systems, Inc., Harvard, Massachusetts, U.S.A. Available from <http://www.vensim.com> . Last accessed October 18, 2020.
6. Nordhaus WD. 1994. *Managing the Global Commons: The Economics of Climate Change*. MIT Press, Cambridge, MA.
7. IPCC, 2013. *Climate Change 2013: The Physical Science Basis*. Contribution of Working Group I to the Fifth Assessment Report of the Intergovernmental Panel on Climate Change. Geneva, Switzerland.
8. King M, Altdorff D, Li P, Galagedara, L, Holden, J, and Unc, A, 2018. Northward shift of the agricultural climate zone under 21 st -century global climate change. *Sci Rep* 8:1–10 . doi: 10.1038/s41598-018-26321-8.
9. National Aeronautics and Space Administration (NASA), 2019. Global Temperature. In: Glob. Land-Ocean Temp. Index. <https://climate.nasa.gov/vital-signs/global-temperature/> . Last accessed October 18 2020.
10. Krinner G, Germany F, Shongwe M, 2013. Long-term climate change: Projections, commitments and irreversibility. *Clim Chang Phys Sci Basis Work Gr I Contrib to Fifth Assess Rep*, Intergov Panel Clim Chang 9781107057:1029–1136 . doi: 10.1017/CBO9781107415324.024